



## Dielectric behaviour of $(\text{Ba}_{0.77}\text{Ca}_{0.23})(\text{Ti}_{0.98}\text{Dy}_{0.02})\text{O}_3$ ceramics

Abdul Moquim, Manas R. Panigrahi\*

*Electroceramics Lab, Department of Physics, School of Applied Sciences, KIIT University, Bhubaneswar-24, Odisha, India*

Received 31 March 2015; Received in revised form 21 May 2015; Received in revised form 17 June 2015;

Accepted 20 June 2015

### Abstract

*In this study,  $\text{BaTiO}_3$  is modified with  $\text{Ca}^{2+}$  and in addition doped with  $\text{Dy}^{3+}$  at the B site lattice. The main idea is to search for new lead-free ferroelectric material and improve their properties. For this purpose, the barium calcium titanate (BCT) as a host and the rare earth element  $\text{Dy}^{3+}$  as an activator were used to fabricate a multifunctional material. The obtained ceramics was found to be homogeneous, dense and a single phase material with no evidence of secondary phases. The dielectric study showed that  $T_C$  increases with the addition of dopants and the obtained ceramics behaves like a relaxor ferroelectric. Some important structural parameters and dielectric properties of dysprosium modified barium (calcium) titanate ceramics are presented.*

**Keywords:** barium calcium titanate, Dy doping, structure, dielectric properties, relaxor ferroelectric

### I. Introduction

Barium titanate ( $\text{BaTiO}_3$ ) is an important ceramic material for electronic and memory devices. The ability of the material to form solid solutions with different dopant ions makes the material versatile for various applications [1]. The solid solubility of the material depends on the site of substitution, charge compensation mechanism involved and solid solubility limit of a dopant. Dopant in the  $\text{BaTiO}_3$  ceramics can occupy either octahedrally coordinated  $\text{Ti}^{4+}$  site or dodecahedrally coordinated  $\text{Ba}^{2+}$  site. There are several reports on the different A site and B site dopants modifying the electrical properties of  $\text{BaTiO}_3$  ceramics [2–6]. In recent years, a considerable amount of work has been done on the ferroelectric properties of  $\text{BaTiO}_3$ . In addition to  $\text{BaTiO}_3$ , there are other different perovskites which have been reported as ferroelectrics [7]. On heating,  $\text{BaTiO}_3$  undergoes a ferroelectric/paraelectric phase transition to the cubic polymorphism at the Curie temperature ( $T_C$ ) of 120 °C. The substitution of iso-valent cations, such as  $\text{Ca}^{2+}$  alter its lattice constant and thereby its dielectric properties. Iso-valent substituted  $\text{BaTiO}_3$  is the potential candidate for various electronic applications and has been actively studied. Among them Ca doped  $\text{BaTiO}_3$  is considered to be one of the important candidate for lead

free electro optic modulators and memory devices [8]. Solid solutions of  $\text{Ba}_{1-x}\text{Ca}_x\text{TiO}_3$  (for  $x = 0.05$  to 0.9) have been widely studied as well as their relaxor nature. The material shows single phase up to  $x = 0.3$  in different study and thereafter it becomes diphasic [9].  $\text{Ca}^{2+}$  has a smaller ionic radius than  $\text{Ba}^{2+}$ . However, it has been pointed out that the Ca ion in  $\text{Ba}_{1-x}\text{Ca}_x\text{TiO}_3$  might have greater atomic polarisability, thereby intensifying the interactions between the Ti ions and, thus, compensate the decrease of  $T_C$ .

Substitution of aliovalent cations in  $\text{BaTiO}_3$  resulted in significant change in electrical properties because of their acceptor/donor behaviour [10]. Trivalent rare earth cations have moderate atomic radii between  $\text{Ba}^{2+}$  and  $\text{Ti}^{4+}$  ions and ability to substitute both A and B site and so they are widely used to modify  $\text{BaTiO}_3$  [11–16].

Ferroelectric materials may be divided into two different classes depending on whether they are normal (classical) or diffuse (relaxor) ferroelectrics [17]. The typical characteristic of the later is that at least two different cations have to be localised in the same crystallographic site. Actually, the  $\text{ABO}_3$  oxide perovskites show fully ordered transitions, mesoscopic disorder leading to the relaxor behaviour and dipolar glass states [18–23]. In addition, to the usual application of the ferroelectric materials, relaxors are of great interest for dielectrics in capacitors and actuators [24]. Relaxor ferroelectrics have been widely studied in recent years due to their remarkable properties and wide prospects of practical

\*Corresponding author: tel: +91 674 2725113,  
fax: +91 674 2725113, e-mail: mrpanigrahi@kiit.ac.in

applications [25,26]. The relaxor ferroelectric generally belongs to the family with mixed cations ferroelectric and perovskite structure with general chemical formula  $AA'BB'O_3$ . Maximum dispersion in relaxor ferroelectric is believed to originate from polar nano regions (PNR) inside which apparent ferroelectric-like order exists.

The most intensively studied relaxor materials are usually lead based ceramics and their derived compounds such as lead magnesium niobate (PMN), lead magnesium niobate-lead titanate (PMN-PT), lead scandium titanate (PST), lead lanthanum zirconate titanate (PLZT) etc. [27,28]. But, because of their volatility and toxicity these materials are becoming undesirable. These days with the recent growing demand of global environmental protection research much attention has been attracted to lead-free environmentally friendly and heavy metal free materials. Researchers have shown their interest in the solid solution system of perovskite  $BaTiO_3$  like, barium zirconium titanate (BZT), barium calcium titanate (BCT), barium magnesium titanate (BMT), barium strontium titanate (BST) etc., with different concentrations of dopants and their combinations i.e. double perovskite system. In the present study an attempt is made to study the relaxor behaviour and the effect of dysprosium at the solid solubility limit of  $Ba_{0.77}Ca_{0.23}TiO_3$  ceramics.

## II. Materials and Methods

Dy modified  $(Ba,Ca)TiO_3$  ceramics were prepared just above its solid solubility limit, i.e.  $Ba_{0.77}Ca_{0.23}TiO_3$ , by conventional solid state reaction (SSR) technique. Stoichiometric proportion high purity powders of  $BaCO_3$  (99.9% pure Merck),  $CaCO_3$  (99.9% pure Merck),  $TiO_2$  (99.9% pure Merck) and  $Dy_2O_3$  (99.9% pure Merck) were grounded for more than 6 h with acetone medium in an agate mortar for homogeneous mixing of powders. The composite powders were conventionally calcined at  $1280^\circ C$  for 4 h in an electrical fur-

nace. Then the calcined powders were once again thoroughly mixed and ground for 2 h, mixed with 2 wt.% of polyvinyl alcohol (PVA) as binder and pressed into disk-shaped pellets of 10 mm diameter and finally the green ceramics were sintered at  $1320^\circ C$  for 6 h.

The ceramics were structurally characterized by an X-ray diffractometer. The X-ray powder diffraction profiles of the samples were recorded using graphite filtered  $CuK\alpha$  radiation from a highly stabilized and automated X-ray generator operated at 30 kV and 20 mA. The data were recorded within the angular range  $10-90^\circ$ . Scanning electron microscopy (SEM) JEOL JSM 6480LV was used for the observation of the microstructure of the ceramics. An electron beam of 10 kV and  $57 \mu A$  was used for the SEM study. For dielectric measurement, both sides of the samples were polished for smooth surfaces to a thickness of 0.7 mm. Electrodes were made by applying silver paste on both sides of the specimen and annealed at  $350^\circ C$  for 5 min. Dielectric measurement was carried out over the frequency range 1 kHz to 1 MHz using an LCR meter connected to PC. The dielectric data was collected at an interval of  $5^\circ C$  while heating at a rate of  $0.5^\circ C$  per min.

## III. Results and discussion

X-ray diffractograms of the prepared  $BaTiO_3$  and  $Ba_{0.77}Ca_{0.23}TiO_3$  ceramics are presented in Figure 1a, whereas XRD pattern of  $Ba_{0.77}Ca_{0.23}Dy_{0.02}Ti_{0.98}O_3$  is shown in Fig. 1b. X-ray analysis, the fingerprint of a material, shows that the investigated ceramics are single phase materials without evidence of any secondary phases. The X-ray parameters are given in Table 1. Detailed X-ray parameters of  $Ba_{0.77}Ca_{0.23}Dy_{0.02}Ti_{0.98}O_3$  ceramic are given in Table 2 including  $hkl$  indices of different planes. For precise structural characterization of a material, it is necessary to understand its flawless crystallographic parameters. Based on these parameters, crystallite size, strain, different peak profile parameters like, peak position, integral breadth, unit cell

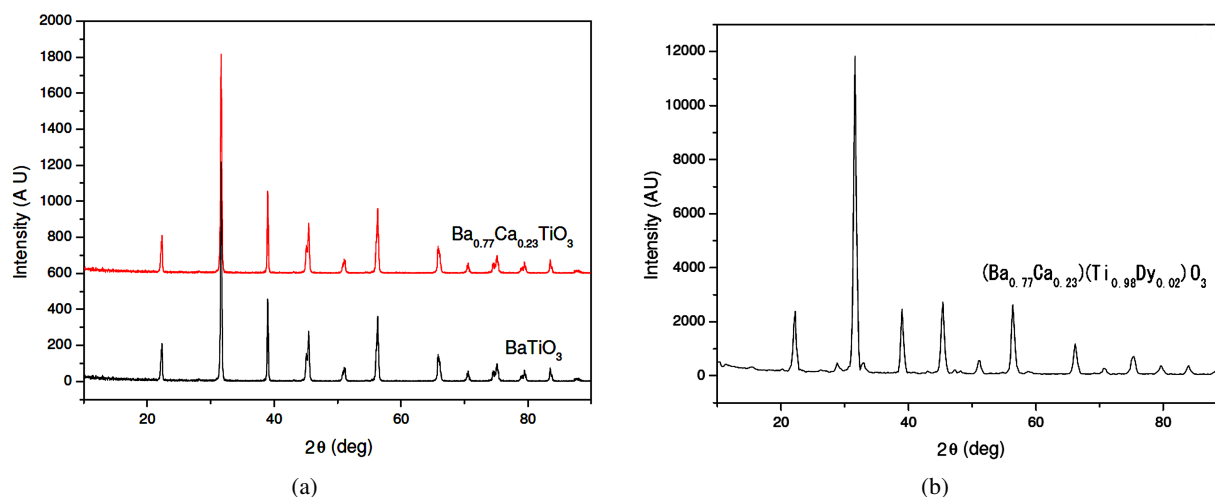


Figure 1. X-ray diffractograms of: a)  $BaTiO_3$ ,  $Ba_{0.77}Ca_{0.23}TiO_3$  and b)  $(Ba_{0.77}Ca_{0.23})(Dy_{0.02}Ti_{0.98})O_3$  ceramics

**Table 1. Compositions of TiN samples obtained by RBS analyses**

Sample	$2\theta$ [°]	$d_{hkl}$ [nm]	FWHM [nm]	$D_{hkl}$ [nm]	lattice strain ( $\epsilon$ )	plastic strain ( $e$ )
I	31.63	0.2827	0.0243	34.02	0	0.88
II	31.89	0.2804	0.0267	30.92	0.008	0.87
III	31.62	0.2839	0.0384	21.33	0.528	0.80

volume, RIR values etc., and different lattice parameters can be estimated. In order to get the detailed X-ray analysis, the X-ray diffractogram was subjected to quantitative X-ray analysis by Rietveld refinement technique. The process involves the removal of overlapping wavelength considering zero shift, and the refinement starts without considering the temperature factor. Crystallographic and size-strain analyses were carried out simultaneously. After convergence of refinement the obtained data are presented in Table 2. The XRD pattern matches with tetragonal barium titanate (ref. ID 980034393) and the following parameters for the studied  $\text{Ba}_{0.77}\text{Ca}_{0.23}\text{Dy}_{0.02}\text{Ti}_{0.98}\text{O}_3$  ceramics were obtained: crystal system – tetragonal; Bravais type – body centred; space group –  $I41/acd$ ;  $a = b = 3.9963(4)\text{Å}$  and  $c = 4.0370\text{Å}$ , with cell volume of  $74.47\text{Å}^3$ . The calculated ( $d_{cal}$ ) and observed ( $d_{obs}$ ) values of inter-planner distances were found to be in good agreement with each other.

Figure 2 shows the scanning electron microscope (SEM) images of  $\text{BaTiO}_3$ ,  $\text{Ba}_{0.77}\text{Ca}_{0.23}\text{TiO}_3$  and  $\text{Ba}_{0.77}\text{Ca}_{0.23}\text{Dy}_{0.02}\text{Ti}_{0.98}\text{O}_3$  ceramics. The microstructure is found to be dense and the grains are uniformly distributed. The sample I ( $\text{BaTiO}_3$ ), has a little bit larger grain sizes than the sample II  $\text{Ba}_{0.77}\text{Ca}_{0.23}\text{TiO}_3$ . This may be attributed to the fact that  $\text{Ca}^{2+}$  acts as grain growth inhibitor and  $\text{Ca}^{2+}$  enters into the sub-lattice of  $\text{Ba}^{2+}$  atoms. But, in the sample III ( $\text{Ba}_{0.77}\text{Ca}_{0.23}\text{Dy}_{0.02}\text{Ti}_{0.98}\text{O}_3$ ) the grain size further increases in the studied range. The ceramo-graphs shows very clear grains and grain boundary. This may be attributed to the reason that,  $\text{Dy}^{3+}$  may be replacing  $\text{Ti}^{4+}$

ions in spite of going into the A-site. The lattice parameter is found to decrease relative to the undoped sample, due to the shrinkage of the unit cell. The unit cell volume is lower ( $64.47\text{Å}^3$ ) compared to the parent sample. Aliovalent substitutions cause a distortion of the lattice. The interactions between B-site ions and  $\text{O}^{2-}$  become stronger resulting in an increase in  $T_C$  and  $\text{Dy}^{3+}$  tends to occupy B sites rather than A-sites. The rare-earth elements, having its  $4f$  orbital totally screened by  $5s$  and  $5p$  orbital, play an important role in deciding the electrical and magnetic properties.

Because of the larger radius, the substitution of  $\text{Dy}^{3+}$  for  $\text{Ti}^{4+}$  in B-sites may depress the oriented displacement of B-site ions in the oxygen octahedrons, which are responsible for the spontaneous polarization. Aliovalent substitutions cause a distortion of the lattice. The interactions between B-site ions and  $\text{O}^{2-}$  become stronger resulting in an increase in  $T_C$  and  $\text{Dy}^{3+}$  tends to occupy B sites rather than A-sites. Because of the larger radius, the substitution of  $\text{Dy}^{3+}$  for  $\text{Ti}^{4+}$  in B-sites may depress the oriented displacement of B-site ions in the oxygen octahedrons, which are responsible for the spontaneous polarization. This is attributed to distortion produced  $\text{Dy}^{3+}$  ions on B-sites, which locally produces deformation in the lattice due to a crystal field potential. This may also be due to atomic mass and volume of the dopant, which affect Dy–O distances on octahedral sites, suggesting that  $\text{Dy}^{3+}$  ions occupied octahedral lattice sites.

Figure 3 shows the temperature dependent dielectric constant ( $\epsilon$ ) of the bulk  $\text{Ba}_{0.77}\text{Ca}_{0.23}\text{Dy}_{0.02}\text{Ti}_{0.98}\text{O}_3$  ceramics at different frequencies (from 1 kHz to 1 MHz).

**Table 2. Structural parameters of  $\text{Ba}_{0.77}\text{Ca}_{0.23}\text{Dy}_{0.02}\text{Ti}_{0.98}\text{O}_3$  ceramics**

No.	Diffraction angle (deg)		FWHM $2\theta$ [°]	Inter planner spacing		Lattice plane $hkl$	Integral breadth $2\theta$ [°]	Crystallite size [nm]	Lattice strain
	$2\theta$ (c) [°]	$2\theta$ (o) [°]		$d_{cal}$ [Å]	$d_{obs}$ [Å]				
1	22.2250	22.1850	0.192	3.9967	4.0038	100	0.96	42.02	1.77
2	31.4809	31.4645	0.384	2.8395	2.8409	101	1.28	21.33	0.528
3	38.8748	38.8515	0.168	2.3148	2.3161	111	1.28	49.58	0.579
4	44.8924	44.8542	0.192	2.0175	2.0191	002	1.28	44.09	0.808
5	45.3461	45.3352	0.192	1.9983	1.9988	200	1.28	44.15	0.225
6	51.0584	51.0310	0.288	1.7874	1.7883	210	0.96	29.96	0.501
7	55.9550	55.9385	0.144	1.6420	1.6424	112	0.96	60.97	0.270
8	56.2455	56.2480	0.192	1.6342	1.6341	211	1.28	45.77	0.041
9	65.7163	65.6984	0.168	1.4197	1.4201	202	0.96	54.37	0.242
10	66.0685	66.0797	0.192	1.4130	1.4128	220	1.28	47.65	0.150
11	70.3082	70.3101	0.384	1.3378	1.3378	212	1.28	24.30	0.023
12	74.3547	74.3660	0.288	1.2747	1.2746	103	1.28	33.07	0.129
13	75.1046	75.0770	0.240	1.2639	1.2642	310	0.96	39.84	0.313
14	79.3876	79.4066	0.384	1.2061	1.2058	311	0.96	25.49	0.120
15	83.4496	83.4811	0.240	1.1574	1.1570	222	1.28	41.76	0.308

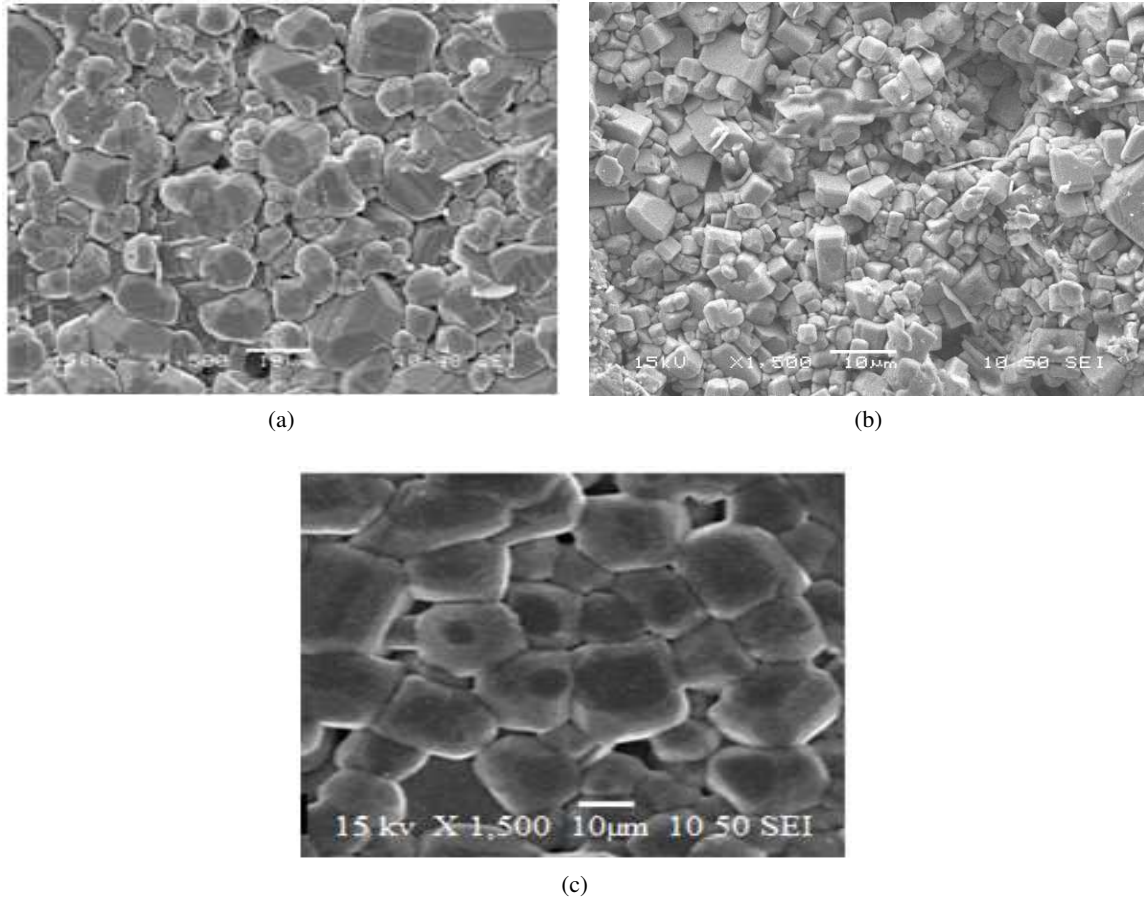


Figure 2. SEM micrographs of: a)  $\text{BaTiO}_3$ , b)  $\text{Ba}_{0.77}\text{Ca}_{0.23}\text{TiO}_3$  and c)  $\text{Ba}_{0.77}\text{Ca}_{0.23}\text{Dy}_{0.02}\text{Ti}_{0.98}\text{O}_3$  ceramics

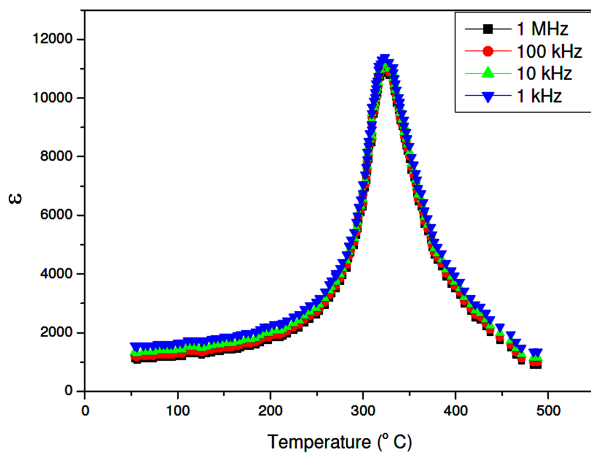
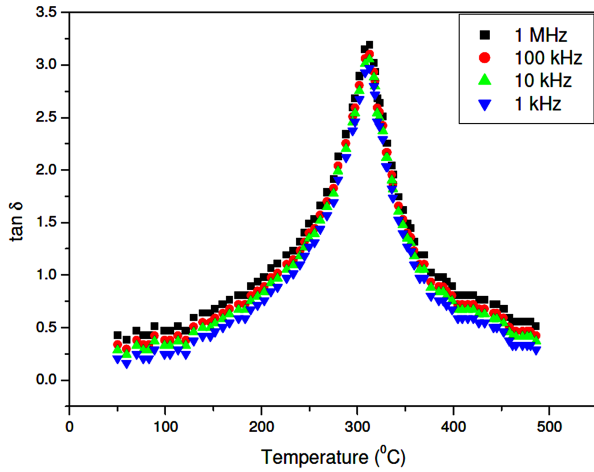


Figure 3. Dielectric constant ( $\epsilon$ ) vs. temperature of  $\text{Ba}_{0.77}\text{Ca}_{0.23}\text{Dy}_{0.02}\text{Ti}_{0.98}\text{O}_3$  ceramics

The value of temperature dependent permittivity increases gradually to maximum value ( $\epsilon_m$ ) with temperature up to the transition temperature and then decreases smoothly indicating a phase transition. The maximum of dielectric permittivity,  $\epsilon_m$ , and the corresponding maximum temperature  $T_m$ , depend upon the measurement frequency. The magnitude of dielectric constant decreases with increase in frequency and the maxima are shifting towards higher temperature. A fre-

quency dispersion takes place for  $T \ll T_m$  and the value of  $\epsilon_m$  decreases when frequency increases. This indicates that the dielectric polarization is of relaxation type in nature. At 1 kHz, the dielectric maximum ( $\epsilon_m$ ) of  $\text{Ba}_{0.77}\text{Ca}_{0.23}\text{Dy}_{0.02}\text{Ti}_{0.98}\text{O}_3$  ceramic and the observed high value of  $T_m$  is due to the higher grain size. The dielectric constant appreciably increases with temperature within the range of 300–400 °C, from which it can be deduced that Dy-doping has caused the existence of a new phase transformation temperature, thereby, changing the polarization and dielectric properties of the ceramics. The high value of the dielectric constant at low frequencies is due to the accumulation of charges at the interfaces between the sample and the electrodes, i.e., Maxwell-Wagner polarization and interfacial polarization. As the frequency increases, the dipoles in the samples reorient themselves fast enough to respond to the applied electric field resulting in the increase in dielectric constant at higher frequencies, which is attributed to the increase in the grain size. The SEM micrographs show more aggregated grains within its microstructure. The increase in dielectric constant as a function of concentration is because of the grain aggregates which induce the internal stress within the grains. When a fine-grained ceramics are subjected to field, the grain is subjected to an internal stress which depends on the orientation of all the surrounding grains. Thus, the in-



**Figure 4. Dielectric constant ( $\tan \delta$ ) vs. temperature of  $\text{Ba}_{0.77}\text{Ca}_{0.23}\text{Dy}_{0.02}\text{Ti}_{0.98}\text{O}_3$  ceramics**

crease in dielectric constant is observed. The stress system would tend to suppress the spontaneous deformation and force the grain back toward the cubic state. As Dy is doped in ceramics, the Curie temperature of ceramics has been shifted toward higher temperature due to the internal stresses developed within the ceramics. Meanwhile, temperature dependant dielectric constant exhibited broad peak indicating the diffuse phase transition. It is reported that as the grain size decreases, the maximum dielectric constant and transition temperature decrease [25]. The temperature and frequency variation of the imaginary part (Fig. 4) of dielectric permittivity shows that, the maximum dielectric temperature shifted to higher values on increasing frequencies. Here the evolution of frequency dispersion is characterized by an increase in dielectric loss when frequency increases. Additionally, there is a deviation from Curie-Weiss law.

It is known that the dielectric permittivity of a normal ferroelectric above the Curie temperature follows the Curie-Weiss law described by:

$$\varepsilon = \frac{C}{(T - T_0)} \quad (T > T_C) \quad (1)$$

where  $T_0$  is the Curie-Weiss temperature and  $C$  is the Curie-Weiss constant. The value of the Curie-Weiss temperature  $T_0$  is greater than that of  $T_m$  and also there is an appreciable difference between the  $T_{dev}$  (401.7 °C) and  $T_m$ . Thus, a strong dielectric dispersion is evidenced leading to Vogel-Fulcher behaviour.

Figure 5 shows the plot of inverse dielectric constant versus temperature at different frequencies. The differ-

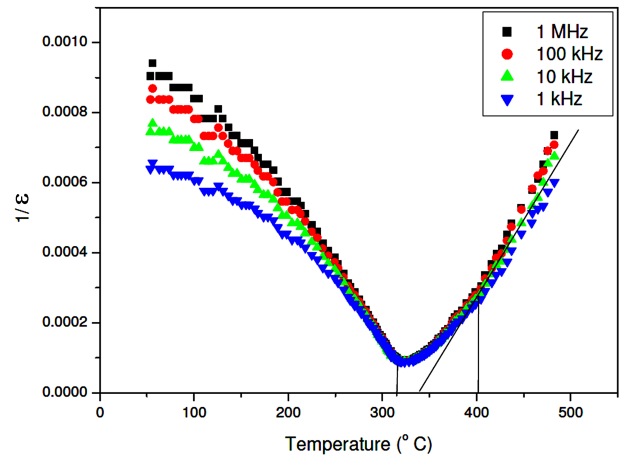


**Figure 5. Inverse dielectric constant ( $1/\varepsilon$ ) vs. temperature of  $\text{Ba}_{0.77}\text{Ca}_{0.23}\text{Dy}_{0.02}\text{Ti}_{0.98}\text{O}_3$  ceramics at different frequencies**

ent parameters obtained are listed in Table 3. The parameter  $\Delta T_m$ , which describes the degree of the deviation from the Curie-Weiss law, is defined as:

$$\Delta T_m = T_{CW} - T_m \quad (2)$$

where  $T_{CW}$  denotes the temperature from which the permittivity starts to deviate from the Curie-Weiss law and  $T_m$  represents the temperature of the dielectric maximum. The Curie temperature is determined from the graph by extrapolation of the reciprocal of dielectric constant of the paraelectric region and the values obtained are given in Table 3.

The diffuse characteristics of ferroelectric-paraelectric phase transition are known to deviate from the typical Curie-Weiss behaviour and can be described by a modified Curie-Weiss relationship [29,30]:

$$\frac{1}{\varepsilon} - \frac{1}{\varepsilon_m} = \frac{(T - T_m)^\gamma}{C} \quad (3)$$

where  $\gamma$  and  $C$  are assumed to be constant. The parameter  $\gamma$  gives information on the character of the phase transition: For  $\gamma = 1$ , a normal Curie-Weiss law is obtained, and  $\gamma = 2$  describes a complete diffuse phase transition [31].

Figure 6 shows the plot of  $\ln(1/\varepsilon - 1/\varepsilon_m)$  vs.  $\ln(T - T_m)$ . The value of  $\gamma$  was found to be 1.9 at frequency 10 kHz (Table 3). Thus, it is clear that, there is a clear diffuse phase transition. The diffuse phase transition and deviation from Curie-Weiss type behaviour may be assumed due to disordering. The diffusiveness occurs

**Table 3. Temperature dependency dielectric parameters of the composition  $\text{Ba}_{0.77}\text{Ca}_{0.23}\text{Dy}_{0.02}\text{Ti}_{0.98}\text{O}_3$  ceramics at different frequencies**

Frequency [kHz]	$\varepsilon_m$	$T_m$ [°C]	$T_0$ [°C]	$T_{CW}$ [°C]	$\Delta T_m$ [°C]	$\gamma$	$C$ [ $10^6$ °C]
1	11452.12	315.6	337.62	344.9	29.3	-	1.78
10	11134.51	317.2	338.71	345.5	28.3	1.9	1.72
100	10977.53	322.96	340.46	346.2	23.24	-	1.67
1000	10816.91	324.23	342.52	347.14	22.9	-	1.63

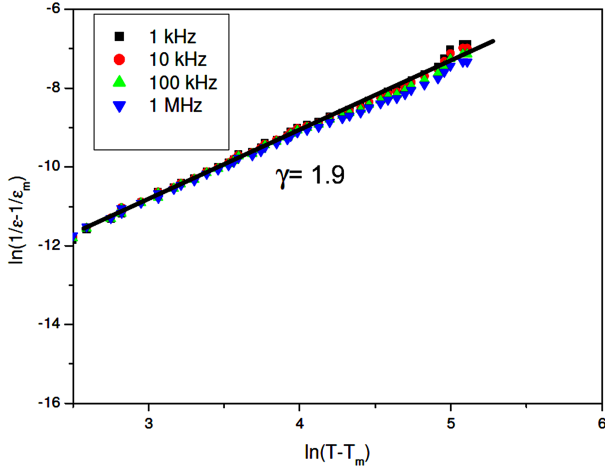


Figure 6.  $\ln(1/\varepsilon - 1/\varepsilon_m)$  vs.  $\ln(T - T_m)$  of  $\text{Ba}_{0.77}\text{Ca}_{0.23}\text{Dy}_{0.02}\text{Ti}_{0.98}\text{O}_3$  ceramics at 1 kHz

mainly due to the compositional fluctuation and structural disordering in the arrangement of cations in one or more crystallographic sites of the structures. The randomly distributed electrical field in a mixed oxide system is reported to be the main reason leading to the relaxor behaviour. Aliovalent cations incorporated in a perovskite lattice have been reported to serve as donors or acceptors, which could affect the electrical characteristics greatly, even though the solubility remained at the trace level.

The broadening of the phase transition is better illustrated by plotting the reduced dielectric constant  $\varepsilon/\varepsilon_m$  as a function of reduced temperature ( $\tau$ ) at different frequencies (Fig. 7). The full width of the plot has very little dispersion over a wide frequency range similar to the observation made in other relaxor materials [32].  $\text{Ba}^{2+}$  ions are replaced by  $\text{Ca}^{2+}$  ions in the first stage, which have a smaller ionic radius. Moreover, aliovalent substitutions cause a distortion of the lattice. The interactions between B-site ions and  $\text{O}^{2-}$  become stronger resulting in an increase in  $T_C$  and  $\text{Dy}^{3+}$  tends to occupy B site rather than A-sites. Because of the larger radius, the

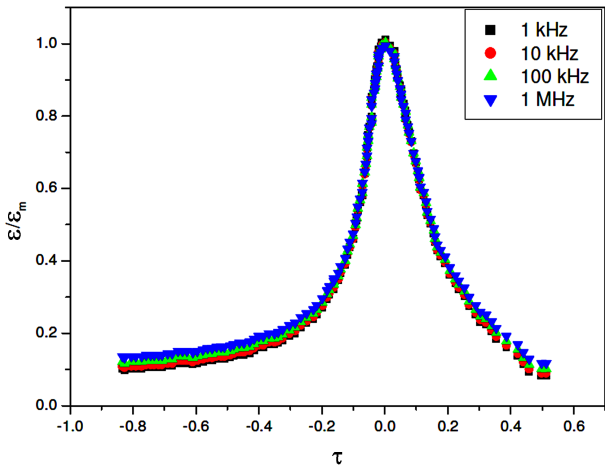


Figure 7. Reduced dielectric constant  $\varepsilon/\varepsilon_m$  as a function of reduced temperature ( $\tau$ ) at different frequencies

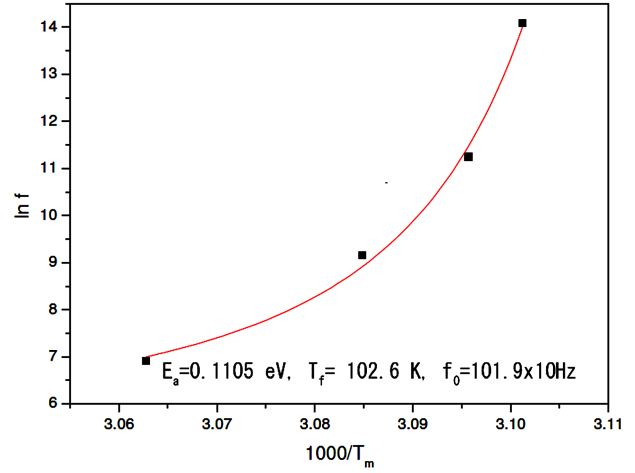


Figure 8.  $\ln f$  vs.  $1000/T_m$  of  $\text{Ba}_{0.77}\text{Ca}_{0.23}\text{Dy}_{0.02}\text{Ti}_{0.98}\text{O}_3$  ceramics at 1 kHz

substitution of  $\text{Dy}^{3+}$  for  $\text{Ti}^{4+}$  in B-sites may depress the oriented displacement of B-site ions in the oxygen octahedrons, which are responsible for the spontaneous polarization. Yet another parameter, which is used to characterize the degree of relaxation behaviour in the frequency range of 100 Hz to 10 kHz, is described by [33]:

$$\Delta T_{relax} = T \cdot \varepsilon_m(100 \text{ kHz}) - T \cdot \varepsilon_m(10 \text{ kHz}) \quad (4)$$

The value of  $\Delta T_{relax}$  was determined to be zero K for the present sample. The above characterization done on the basis of Curie-Weiss law and the value of empirical parameters like  $\Delta T_m$ ,  $\gamma$ , and  $\Delta T_{relax}$  suggest that the permittivity of  $\text{Ba}_{0.77}\text{Ca}_{0.23}\text{Dy}_{0.02}\text{Ti}_{0.98}\text{O}_3$  ceramic follows Curie-Weiss law only at temperatures much higher than  $T_m$ . Thus, the large deviation from the Curie-Weiss type behaviour, large relaxation temperature  $\Delta T_{relax}$ , and  $\gamma = 1.9$ , suggest also that  $\text{Ba}_{0.77}\text{Ca}_{0.23}\text{Dy}_{0.02}\text{Ti}_{0.98}\text{O}_3$  is a relaxor ferroelectric.

The frequency dependency of  $T_m$  is shown in Fig. 8 as  $\ln f$  vs.  $1000/T_m$ . The observed frequency dependence of  $T_m$  was empirically evaluated using Vogel-Fulcher's relation and computed using the following equation:

$$\log f = \log f_0 - \frac{E_a}{k_B(T_m - T_{vf})} \quad (5)$$

where  $f_0$  is the high temperature extrapolation of the attempt frequency,  $E_a$  is the measurement of average activation energy,  $k_B$  the Boltzman constant,  $T_{vf}$  the static freezing temperature of polarization fluctuation and  $f$  is the pre exponential factor. All these dielectric characteristics are typical for relaxor behaviour. The fitting parameters for the compositions are found to be,  $E_a = 0.1105 \text{ eV}$ ,  $T_f = 102.6 \text{ K}$ ,  $f_0 = 101.9 \times 10^4 \text{ Hz}$ . The fitting parameters having close agreement with the data of Vogel-Fulcher's relation suggests that the relaxor behaviour in the system is analogous to that of a dipolar glass with polarization fluctuations above a static freezing temperature.

#### IV. Conclusions

The perovskite  $\text{Ba}_{0.77}\text{Ca}_{0.23}\text{Dy}_{0.02}\text{Ti}_{0.98}\text{O}_3$  ceramics was prepared through a solid state reaction route. The room temperature XRD study suggests that the composition has a single phase in teragonal symmetry. The dielectric study of the compositions shows a typical relaxor like behaviour. The relaxor behaviour observed in this ceramics can be induced by many reasons, such as microscopic compositions fluctuation, the merging of micro-polar regions into macro-polar regions, or a coupling of the order parameter and the local disorder mode through the local strain. In perovskite-type compounds the relaxor behaviour appears when at least two cations occupy the same crystallographic sites A or B. Both Ti and Dy are ferroelectrically active and these cations are off-centred in the octahedral site giving rise to a local dipolar moment. A quantitative characterization of the relaxor behaviour based on the empirical parameters ( $\Delta T_m$ ,  $\Delta T_{res}$ , and  $\Delta T_{CW}$ ) confirms the relaxor behaviour of  $\text{Ba}_{0.77}\text{Ca}_{0.23}\text{Dy}_{0.02}\text{Ti}_{0.98}\text{O}_3$  composition. In addition, there is a strong deviation from Curie-Weiss law. A deviation for  $T < T_{dev}$  is the characteristic of dipole interactions responsible for some type of short range order. The large curvature of  $1/\epsilon$  around  $T_m$  is in good agreement with a strongly diffuse phase transition.

#### References

1. B. Jaffe, W.R. Cook, H. Jaffe, *Piezoelectric Ceramics*, Academic Press, London, 1971.
2. X.S. Wang, C.N. Xu, H. Yamada, "Large electrostriction near the solubility limit in  $\text{BaTiO}_3$ - $\text{CaTiO}_3$  ceramics", *Appl. Phys. Lett.*, **86** (2005) 022905 (1–3).
3. X.S. Wang, C.N. Xu, H. Yamada, "Electro-mechano-optical conversions in  $\text{Pr}^{3+}$ -doped  $\text{BaTiO}_3$ - $\text{CaTiO}_3$  ceramics", *Adv. Mater.*, **17** (2005) 1254–1258.
4. M.C. McQuarrie, F.W. Behnke, "Structural and dielectric studies in the system  $(\text{Ba,Ca})(\text{Ti,Zr})\text{O}_3$ ", *J. Am. Ceram. Soc.*, **37** (1954) 539–543.
5. R.C. DeVries, R. Roy, "Phase equilibrium in the system  $\text{BaTiO}_3$ - $\text{CaTiO}_3$ ", *J. Am. Ceram. Soc.*, **38** (1955) 158–171.
6. E. Brucsu, G. Ravichandran, K. Bhattacharya, "Large strain electrostrictive actuation in barium titanate", *Appl. Phys. Lett.*, **77** (2000) 1698–1700.
7. V.G. Bhide, K.G. Deshmukh, M.S. Hegde, "Ferroelectric properties of  $\text{PbTiO}_3$ ", *Physica*, **28** (1962) 871–876.
8. H. Veenhuis, T. Borger, K. Piethmann, M. Flaspohler, K. Buse, "Light-induced charge-transport properties of photorefractive barium-calcium-titanate crystals doped with rhodium", *Appl. Phys. B: Laser Optics*, **70** (2000) 797–801.
9. M.R. Panigrahi, S. Panigrahi, "Diffuse phase transition and dielectric study in  $\text{Ba}_{0.95}\text{Ca}_{0.05}\text{TiO}_3$  ceramic", *Physica B: Condens. Mat.*, **405** (2010) 2256–2259.
10. M.T. Buscaglia, V. Buscaglia, M. Viviani, P. Nanni, M. Hanuskova, "Influence of foreign ions on the crystal structure of  $\text{BaTiO}_3$ ", *J. Eur. Ceram. Soc.*, **20** (2000) 1997–2007.
11. Y. Tsur, A. Hitomi, I. Scrymgeour, C.A. Randall, "Site occupancy of rare earth cations in  $\text{BaTiO}_3$ ", *Jpn. J. Appl. Phys.*, **40** (2001) 255–258.
12. Y. Tsur, T.D. Dunbar, C.A. Randall, "Crystal and defect chemistry of rare earth cations in  $\text{BaTiO}_3$ ", *J. Electroceram.*, **7** (2001) 25–34.
13. J.H. Hwang, Y.H. Han, "Dielectric properties of erbium doped barium titanate", *Jpn. J. Appl. Phys.*, **40** (2001) 676–679.
14. Y. Pu, W. Chen, S. Chen, H.T. Langhammer, "Grain boundary reoxidation of barium titanate ceramics doped with lanthum", *Ceramica*, **51** (2005) 214–218.
15. N.V. Dergunova, E.G. Fesenko, V.P. Sakhnenko, "Rendering barium titanate semiconductive by doping with rareearth elements", *Ferroelectrics*, **83** (1988) 187–191.
16. D. Hreniak, W. Strek, J. Chmielowiec, G. Pasciak, R. Pazik, S. Gierlotka, W. Lojkowski, "Preparation and conductivity measurement of Eu doped  $\text{BaTiO}_3$  nanoceramic", *J. Alloy Compd.*, **408** (2008) 637–640.
17. L.E. Cross, "Relaxor ferroelectrics: An overview", *Ferroelectrics*, **151** (1994) 305–320.
18. G.A. Smolensky, "Physical phenomena in ferroelectrics with diffused phase transitions", *J. Phys. Soc. Jpn.*, **28** (1970) 26–37.
19. L.E. Cross, "Relaxor ferroelectrics", *Ferroelectrics*, **76** (1987) 241–267.
20. B.E. Vugmeister, M.D. Glinchuk, "Dipole glass and ferroelectricity in random-site electric dipole systems", *Rev. Mod. Phys.*, **52** (1990) 993–1026.
21. U.T. Hochli, K. Knorr, A. Loidl, "Orientational glasses", *Adv. Phys.*, **39** (1990) 405–615.
22. M. Maglione, U.T. Hochli, J. Joffrin, "Dipolar glass state in  $\text{K}_{1-x}\text{Na}_x\text{TaO}_3$ ", *Phys. Rev. Lett.*, **57** (1986) 436–439.
23. A. Simon, J. Ravez, M. Maglione, "Relaxor properties of  $\text{Ba}_{0.9}\text{Bi}_{0.067}(\text{Ti}_{1-x}\text{Zr}_x)\text{O}_3$  ceramics", *Solid State Sci.*, **7** (2005) 925–930.
24. K. Uchino, "Relaxor ferroelectric devices", *Ferroelectrics*, **151** (1994) 321–330.
25. S.E. Hao, L. Sun, J.X. Huang, "Preparation and dielectric properties of Dy, Er-doped  $\text{BaZr}_{0.2}\text{Ti}_{0.8}\text{O}_3$  ceramics", *Mater. Chem. Phys.*, **109** (2008) 45–49.
26. H.P. Jeon, S.K. Lee, S.W. Kim, D.K. Choi, "Effects of  $\text{BaO-B}_2\text{O}_3$ - $\text{SiO}_2$  glass additive on densification and dielectric properties of  $\text{BaTiO}_3$  ceramics", *Mater. Chem. Phys.*, **94** (2005) 185–189.
27. H. Khemakhem, A. Simon, J. Ravez, "Relaxor or classical ferroelectric behaviour in ceramics with composition  $\text{Ba}_{1-x}\text{Na}_x\text{Ti}_{1-x}\text{Nb}_x\text{O}_3$ ", *J. Phys.: Condens. Mat.*, **12** (2000) 5951–5955.
28. A. Simon, J. Ravez, "New lead-free non-stoichiometric perovskite relaxor ceramics derived

- from BaTiO<sub>3</sub>”, *Solid State Sci.*, **5** (2003) 1459–1464.
29. X. G. Tang, J. Wang, X. X. Wang, H. L. W. Chan, “Effects of grain size on the dielectric properties and tunabilities of sol-gel derived Ba(Zr<sub>0.2</sub>Ti<sub>0.8</sub>)O<sub>3</sub> ceramics”, *Solid State Com.*, **131** (2004) 163–168.
30. Z. Q. Zhuang, M. P. Harmer, D. M. Smyth, R. E. Newnham, “The effect of octahedrally-coordinated calcium on the ferroelectric transition of BaTiO<sub>3</sub>”, *Mater. Res. Bul.*, **22** (1987) 1329–1335.
31. M.R. Panigrahi, S. Panigrahi, “Ferroelectric relaxor behavior in Ba<sub>0.925</sub>Dy<sub>0.075</sub>TiO<sub>3</sub> ceramic”, *J. Electroceram.*, **26** (2011) 78–83.
32. M. Tyunina, J. Levoska, A. Sternberg, S. Leppavuori, “Dielectric properties of pulsed laser deposited films of PbMg<sub>1/3</sub>Nb<sub>2/3</sub>-PbTiO<sub>3</sub> and PbSc<sub>1/2</sub>Nb<sub>1/2</sub>O<sub>3</sub>-PbTiO<sub>3</sub> relaxor ferroelectrics”, *J. Appl. Phys.*, **86** (1999) 5179–5184.
33. C. Ang, Z. Jing, Z. Yu, “Ferroelectric relaxor Ba(Ti,Ce)O<sub>3</sub>”, *J. Phys.: Condens. Mat.*, **14** (2002) 8901–8912.